AR-KAN: Autoregressive-Weight-Enhanced Kolmogorov-Arnold Network for Time Series Forecasting

Chen Zeng, Tiehang Xu, and Qiao Wang, *Senior Member, IEEE*

Abstract—Traditional neural networks struggle to capture the spectral structure of complex signals. Fourier neural networks (FNNs) attempt to address this by embedding Fourier series components, yet many real-world signals are almost-periodic with non-commensurate frequencies, posing additional challenges. Building on prior work[41] showing that ARIMA outperforms large language models (LLMs) for forecasting, we extend the comparison to neural predictors and find ARIMA still superior. We therefore propose the Autoregressive-Weight-Enhanced Kolmogorov–Arnold Network (AR-KAN), which integrates a pre-trained AR module for temporal memory with a KAN for nonlinear representation. The AR module preserves essential temporal features while reducing redundancy. Experiments demonstrate that AR-KAN matches ARIMA on almost-periodic functions and achieves the best results on 72% of Rdatasets series, with a clear advantage on data with periodic structure. These results highlight AR-KAN as a robust and effective framework for time series forecasting. Our code is available at *https://github.com/ChenZeng001/AR-KAN*.

Index Terms—Time series forecasting, ARIMA, Kolmogorov-Arnold Network, KAN, Almost periodic functions

I. INTRODUCTION

Time series forecasting is a fundamental task in signal processing[1][2], statistics[3], and numerous applied fields, including economics[4], meteorology[5], and healthcare[6]. Among classical approaches, the Autoregressive Integrated Moving Average (ARIMA) model[7] stands out as one of the most influential and widely adopted methods, because it integrates autoregression, differencing, and moving average elements to provide a comprehensible and effective approach for handling practical time series data, even when the time series is non-stationary.

Apart from the aforementioned statistics or Fourier analysis-based methods, neural networks have been utilized in time series forecasting for many years[8], with the goal of enabling the modeling of complex nonlinear dependencies. Architectures such as Multi-Layer Perceptrons (MLPs)[10] and Recurrent Neural Networks (RNNs)[11], particularly Long Short-Term Memory (LSTM) networks[12], have been widely studied. In recent years, Transformer-based models[13][14][15] have gained popularity due to their self-attention mechanism and parallel processing capabilities. Meanwhile, state space

Both C. Zeng and T. Xu was with the School of Information Science and Engineering, Southeast University, Nanjing, China (email: chenzeng@seu.edu.cn, 220250920@seu.edu.cn).

Q. Wang was with both the School of Information Science and Engineering and the School of Economics and Management, Southeast University, Nanjing, China (Corresponding Author, email: qiaowang@seu.edu.cn).

models like Mamba[16] have emerged as efficient alternatives to attention mechanisms, offering linear-time computation and strong performance on long-range sequences. More recently, Kolmogorov-Arnold Networks (KANs)[17][18] have been introduced as a novel architecture with high expressivity and flexible modeling of nonlinear mappings. In parallel, the rapid progress of large language models (LLMs) has led to approaches such as LLMTime[42] and Time-LLM[19], which adapt pretrained language models to temporal tasks by leveraging their strong generalization and sequence modeling capabilities.

In the context of neural forecasting, a specialized research focuses on spectral analysis through specific networks, such as Fourier Neural Networks (FNNs)[20]. These models incorporate Fourier series to enhance spectral modeling[21]. Representative examples include the Fourier Neural Operator (FNO)[23] and the Fourier Analysis Network (FAN)[22], which have been applied to physics-informed learning, partial differential equation solving, and time series prediction.

Nevertheless, these neural network models grounded in representation by Fourier series may overlook a key theoretical constraint: the additive combination of periodic elements does not necessarily result in a periodic function[24][25]. Throughout history, this important topic prompted N. Wiener to create the renowned Generalized Harmonic Analysis (GHA) theory, which works alongside the spectral analysis of time series. When the constituent frequencies are incommensurable, the resulting signal is almost-periodic[26], meaning that it exhibits recurrence without strict periodicity. Empirical studies show that for such signals, even advanced neural models, including FNNs, are often outperformed by classical ARIMA[27][28] and an evaluation could be referred as to our recent work [41].

Empirical studies indicate that, for such signals, even advanced neural models such as FNNs are often outperformed by classical ARIMA methods [27][28]. A more detailed evaluation can be found in our recent work [41].

To address this, we propose AR-KAN, a hybrid model that integrates the strengths of traditional and modern approaches. Based on the Universal Myopic Mapping Theorem[29][30], AR-KAN employs a KAN as the static nonlinear component, while introducing memory through a pre-trained autoregressive (AR) model. This design enables AR-KAN to combine the adaptability and expressiveness of KANs with the strong spectral bias inherent in traditional AR models. Furthermore, the AR memory module itself is a data-driven model whose weights are not fixed but are adaptively determined by the

characteristics of the data. Additionally, it can be shown that when handling time series forecasting tasks, this module effectively eliminates redundancy while retaining the maximal amount of useful information. This property allows the model to flexibly adapt to various temporal patterns without manual intervention.

Extensive experiments demonstrate AR-KAN's effectiveness. On almost-periodic functions, it matches ARIMA's performance. And on real-world datasets from Rdatasets[40], it outperforms baselines on 72% of tasks. The few cases where AR-KAN does not dominate correspond mostly to datasets with weak or nearly absent periodicity, which are inherently difficult to forecast without additional prior information. When focusing on datasets with stronger periodic components, AR-KAN shows a clear and consistent advantage, highlighting its robustness, adaptability, and potential as a unified framework for time series forecasting.

The structure of this paper is organized as follows:

Section II introduces the background, including time series forecasting tasks, ARIMA, MLP, and KAN models. Section III presents the Universal Myopic Mapping Theorem and explains how it inspires the overall architecture of our AR-KAN model. Section IV describes the experiments conducted to demonstrate the effectiveness and generalizability of AR-KAN, including evaluations on two constructed almost-periodic functions and real-world time series. Finally, Section V concludes the paper.

II. BACKGROUND

A. Time Series Forecasting and ARIMA

Time series forecasting aims to predict a sequence based on its past observations. Formally, given a univariate time series $\{x_n\}_{n=1}^T$, the forecasting problem involves learning a mapping $\mathcal{F}$ such that:

$$\hat{x}_{n+h} = \mathcal{F}(x_n, x_{n-1}, \ldots, x_{n-p+1}), \quad (1)$$

where $\hat{x}_{n+h}$ denotes the forecast for h-steps ahead ($h = 1$ in this paper), and p is the order of historical dependence. This formulation can be extended to multivariate or probabilistic settings, but the central challenge remains: capturing the underlying temporal dynamics, dependencies, and possibly noise in the observed data.

A classical and widely used model for time series forecasting is ARIMA. ARIMA is particularly effective for stationary or differenced stationary processes. The general form of an ARIMA(p, d, q) model is given by:

$$\Phi(B)(1 - B)^d x_n = \Theta(B)\epsilon_n, \quad (2)$$

where:

- B is the backshift operator, i.e., $B^k x_n = x_{n-k}$,
- $\Phi(B) = 1 - a_1 B - \cdots - a_p B^p$ is the autoregressive (AR) polynomial of order p,
- $\Theta(B) = 1 + b_1 B + \cdots + b_q B^q$ is the moving average (MA) polynomial of order q,
- d is the degree of differencing to ensure stationarity,
- ϵ_n is assumed to be white noise: $\epsilon_t \sim \mathcal{N}(0, \sigma^2)$.

The integration component $(1 - B)^d$ transforms non-stationary series into stationary ones by differencing. The ARIMA model captures linear temporal dependencies and is known for its statistical interpretability and relatively low computational cost. Despite its simplicity, ARIMA remains a strong baseline in many practical applications, especially when the underlying signal exhibits regular, stationary behavior.

B. MLP and KAN

MLP is one of the most fundamental architectures in neural networks. An MLP consists of multiple layers of affine transformations followed by pointwise nonlinear activations. Given an input $x \in \mathbb{R}^d$, an L-layer MLP computes:

$$f_{\text{MLP}}(x) = W^{(L)}\sigma_{L-1} \cdots \sigma_1 \left(W^{(1)}x + b^{(1)} \right) + b^{(L)}, \quad (3)$$

where $W^{(\ell)}$, $b^{(\ell)}$ are learnable parameters, and σ_ℓ denotes the nonlinear activation at layer ℓ.

However, MLPs exhibit a well-known spectral bias[31], meaning they tend to learn low-frequency components of the target function earlier and more accurately than high-frequency components. While this inductive bias can be beneficial in some applications, it limits the ability of MLPs to capture fine-grained or oscillatory patterns in data.

To overcome the limited expressiveness of fixed activation functions in traditional MLPs, KANs have been proposed as a more flexible and interpretable alternative. KANs are inspired by the Kolmogorov–Arnold representation theorem[32], which states that any multivariate continuous function $f : [0, 1]^d \to \mathbb{R}$ can be expressed as a finite composition of univariate continuous functions:

$$f(x_1, \ldots, x_d) = \sum_{q=1}^{2d+1} \phi_q \left(\sum_{i=1}^d \psi_{qi}(x_i) \right), \quad (4)$$

where ϕ_q and ψ_{qi} are univariate continuous functions. Inspired by this constructive result, KANs replace the fixed nonlinear activations in MLPs with learnable univariate functions, typically represented by splines.

Given an input $x \in \mathbb{R}^d$, an L-layer KAN computes:

$$f_{\text{KAN}}(x) = \Phi^{(L)}\Psi^{(L-1)} \cdots \Psi^{(1)}(x), \quad (5)$$

where each layer $\Psi^{(\ell)} : \mathbb{R}^{d_\ell} \to \mathbb{R}^{d_{\ell+1}}$ is defined by:

$$[\Psi^{(\ell)}(x)]_j = \sum_{i=1}^{d_\ell} w_{ij}^{(\ell)} \cdot \psi_{ij}^{(\ell)}(x_i), \quad (6)$$

and $\Phi^{(L)}$ denotes the final output transformation, typically of the same form. Here, each $\psi_{ij}^{(\ell)}$ is a learnable univariate function, often implemented using splines, and $w_{ij}^{(\ell)}$ are learnable scalar weights.

Unlike MLPs, KANs do not exhibit a low-frequency spectral bias [33]. This enables them to capture high-frequency and oscillatory components more effectively, making them well suited for modeling time series with rich spectral structures.

However, this advantage can also introduce challenges. Without a low-frequency bias, KANs tend to be more sensitive
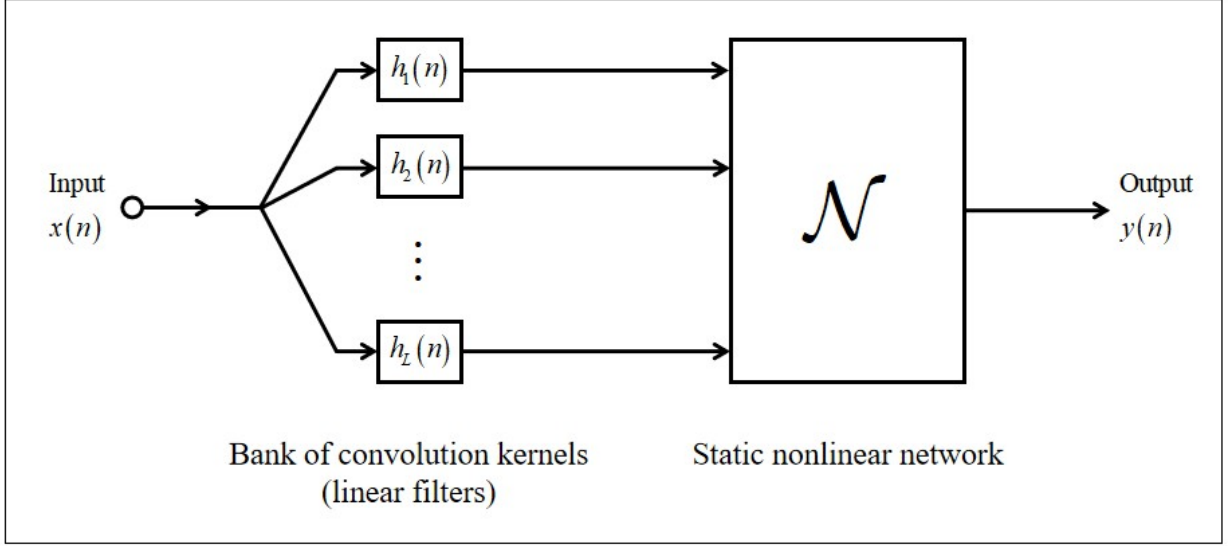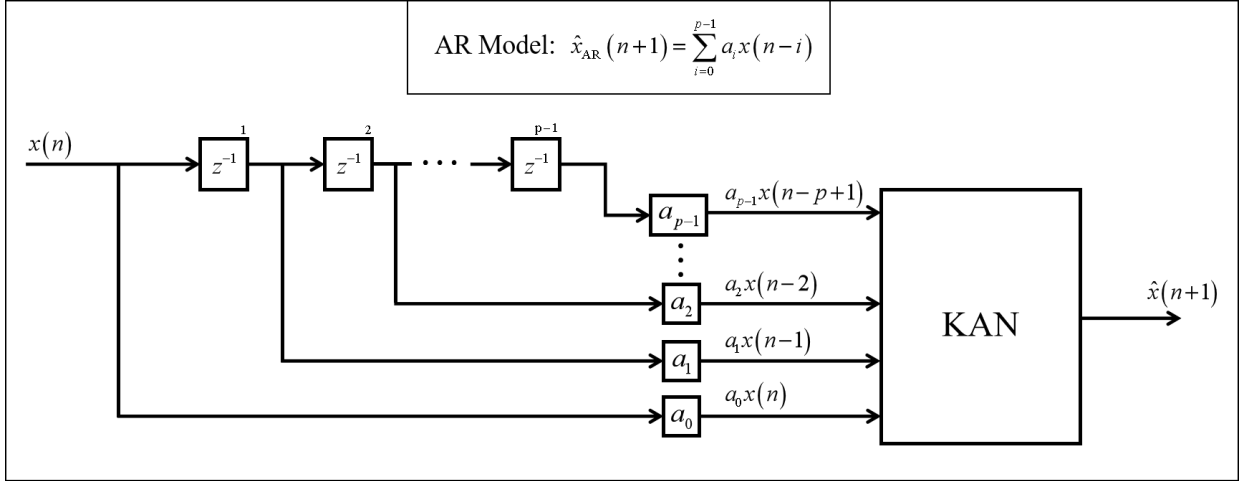
Fig. 1: Universal Myopic Mapping Theorem.

Fig. 2: Model Structure of AR-KAN.

to high-frequency noise[34] and may have difficulty learning functions with limited regularity[35]. In such cases, the model may overfit to spurious variations or become unstable during training.

Nevertheless, in most real-world time series, especially those with structured periodicity, seasonal trends, or non-stationary high-frequency patterns, this characteristic is beneficial. The ability of KANs to model a broad spectrum of frequency behaviors often leads to better performance compared to MLPs.

III. AR-KAN

AR-KAN is derived from the Universal Myopic Mapping Theorem. Therefore, in this section, we first introduce the Universal Myopic Mapping Theorem, then followed by a detailed explanation of the AR-KAN model architecture.

A. Universal Myopic Mapping Theorem

The Universal Myopic Mapping Theorem [29][30] provides a powerful theoretical guarantee for modeling dynamic systems using shallow, feedforward structures. Specifically, it states that any shift-invariant and myopic dynamical map can be uniformly approximated arbitrarily well by a two-stage architecture: a bank of linear filters followed by a static nonlinear mapping, as shown in Fig. 1.

Theorem 1 (Universal Myopic Mapping Theorem [29][30]). *Let $\mathcal{M}$ be a shift-invariant and myopic dynamical system that maps a real-valued time series $\{x_n\}_{n\in\mathbb{Z}}$ to outputs $\{y_n\}$ via a causal and bounded operator. Then, for any $\varepsilon > 0$, there exists a finite collection of linear filters $\{h_i\}_{i=1}^{N}$ and a continuous static nonlinear function $f_\theta : \mathbb{R}^N \to \mathbb{R}$ such that the approximation*

$$y_n \approx f_\theta \left((h_1 * x)_n, (h_2 * x)_n, \ldots, (h_N * x)_n \right)$$

satisfies

$$\sup_n |y_n - f_\theta((h_1 * x)_n, \ldots, (h_N * x)_n)| < \varepsilon,$$

where $*$ denotes convolution and $(h_i * x)_n = \sum_\tau h_i(\tau)x_{n-\tau}$.

This theorem establishes that it is theoretically sufficient to model a wide class of dynamical systems using a finite bank of linear filters followed by a nonlinear function, without requiring recurrent or deep sequential architectures. The key property of myopia means that each output depends only on a bounded past history, and shift-invariance ensures time-homogeneity.

B. Model Structure of AR-KAN

Inspired by the Universal Myopic Mapping Theorem, we design the AR-KAN as a two-stage architecture composed of a data-driven memory module and a static nonlinear mapping, as illustrated in Fig. 2. The static nonlinear network is implemented using a KAN, which has been discussed in Section II to possess stronger spectral modeling capabilities than traditional MLPs, particularly for high-frequency signals. For the memory module, we adopt a pre-trained AR model to serve as the bank of linear filters, effectively incorporating the strengths of classical linear time series models into our architecture.

The memory module operates in the following manner: we first train an AR model from the input time series $\{x(n)\}$ to predict the next step via

$$\hat{x}(n+1) = \sum_{i=0}^{p-1} a_i x(n-i), \tag{7}$$

where p is the AR order and $\{a_i\}_{i=0}^{p-1}$ are the learned AR coefficients. These coefficients are then extracted to define a set of fixed linear filters. At each time step n, a delay buffer forms the historical input vector $\{x(n-i)\}_{i=0}^{p-1}$, which is multiplied elementwise with the corresponding $\{a_i\}_{i=0}^{p-1}$ and passed to the subsequent KAN module. This structure is equivalent to setting the impulse response of the i-th filter in Fig. 1 as:

$$h_i(n) = a_i \delta(n-i), \quad 0 \le i \le p-1, \tag{8}$$

where $\delta(\cdot)$ is the Kronecker delta function.

To express the AR coefficients $\{a_i\}$ explicitly in terms of the time series $\{x(n)\}$, we can solve the Yule–Walker equations[36][37]. Specifically, let $\mathbf{a} = [a_0, a_1, \ldots, a_{p-1}]^\top$ be the coefficient vector, $\mathbf{r} = [r(1), r(2), \ldots, r(p)]^\top$ the autocorrelation vector, and $\mathbf{R}$ the $p \times p$ autocorrelation matrix given by

$$\mathbf{R} = \begin{bmatrix} r(0) & r(1) & \cdots & r(p-1) \\ r(1) & r(0) & \cdots & r(p-2) \\ \vdots & \vdots & \ddots & \vdots \\ r(p-1) & r(p-2) & \cdots & r(0) \end{bmatrix}, \tag{9}$$

then the AR coefficients are computed via:

$$\mathbf{a} = \mathbf{R}^{-1}\mathbf{r}. \tag{10}$$

Here, the autocorrelation function $r(i)$ is defined as

$$r(i) = \mathbb{E}[x(n)\,x(n-i)], \tag{11}$$

or, in practice, estimated from the empirical data as

$$r(i) \approx \frac{1}{N-i} \sum_{n=i}^{N-1} x(n)\,x(n-i), \tag{12}$$

where N is the total number of available samples.

This formulation reveals a key feature of our memory module: the filter weights $\{a_i\}$ are not fixed parameters, but are derived from the underlying data through statistical estimation. In contrast to static memory schemes such as tapped-delay lines[38] or gamma memory[39], our data-driven design allows the memory module to adapt flexibly to the autocorrelation structure of different time series.

C. Analysis of the AR Memory Module

To further elucidate the advantage of the AR memory module, we provide a theoretical analysis demonstrating that it optimally preserves useful information while eliminating redundancy. Consider a general linear memory module with output:

$$y_i(n) = w_i x(n-i), \quad 0 \le i \le p-1, \tag{13}$$

where w_i are the weights.

We aim to maximize the total correlation between the memory outputs and the target $x(n+1)$, which represents the useful information captured:

$$\max \sum_{i=0}^{p-1} \mathbb{E}[y_i(n)x(n+1)]. \tag{14}$$

However, this objective alone is insufficient, as it can be trivially maximized by arbitrarily increasing the magnitude of w_i, which would also amplify noise and irrelevant components. To prevent this and encourage the memory to focus on the most informative features, we introduce a constraint on the total output energy of the memory module:

$$\min \mathbb{E}\left[\left(\sum_{i=0}^{p-1} y_i(n)\right)^2\right]. \tag{15}$$

This constraint penalizes high-energy outputs, effectively forcing the memory to represent the target using a compact set of features and discard redundant information. We combine these two objectives into a single optimization goal:

$$L = \sum_{i=0}^{p-1} \mathbb{E}[y_i(n)x(n+1)] - \frac{1}{2}\mathbb{E}\left[\left(\sum_{i=0}^{p-1} y_i(n)\right)^2\right]. \tag{16}$$

To find the optimal weights that maximize L, we solve $\frac{\partial L}{\partial \mathbf{w}} = 0$ for $\mathbf{w} = [w_0, w_1, \ldots, w_{p-1}]^\top$ gives:

TABLE I: Test loss (MSE) of various models on Noisy Almost Periodic Functions

functions	σ	ARIMA	AR-KAN	AR-MLP	KAN	MLP	Transformer	LSTM	Mamba	FAN	FNO
f_1	0.1	**0.0142**	*0.0203*	0.0270	0.1507	0.1216	0.0584	0.0743	0.1194	0.1173	0.0767
	0.2	**0.0550**	*0.0770*	0.0959	0.1946	0.1273	0.3903	0.1462	0.2934	0.4266	0.1305
	0.3	**0.1206**	*0.1681*	0.1999	0.2947	0.2408	0.4635	0.5209	0.3781	0.7023	0.1979
	0.4	**0.2155**	*0.2892*	0.3543	0.6241	1.4625	1.5572	0.3932	0.5932	0.7965	0.7865
f_2	0.1	*0.0194*	**0.0193**	0.0214	0.0515	0.1525	0.0947	0.0813	0.1149	0.0384	0.0322
	0.2	*0.0881*	**0.0724**	0.0922	0.2812	0.1550	0.5346	0.2424	0.2593	0.5109	0.2747
	0.3	*0.1647*	**0.1593**	0.1745	0.2577	0.6787	1.2197	0.4042	0.5592	0.3506	0.4277
	0.4	*0.3108*	**0.2769**	0.3341	0.7100	1.1827	3.8209	0.4932	0.5914	0.7702	1.1133

Note: Bold numbers indicate the **minimum** value in each row; italic numbers indicate the *second minimum* value.
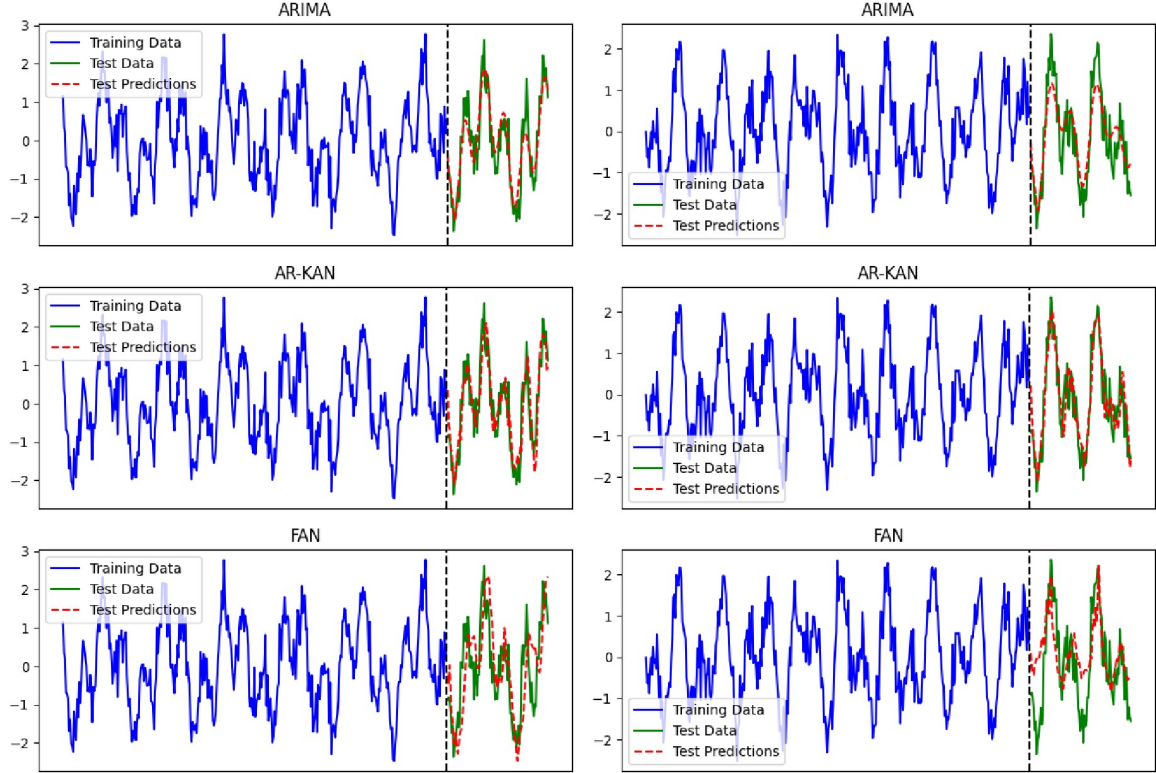

Fig. 3: Performance of ARIMA, AR-KAN and FAN on Noisy Almost Periodic Functions, $\sigma = 0.4$ (left: f_1, right: f_2).

$$\mathbf{w}^* = \mathbf{R}^{-1}\mathbf{r}, \tag{17}$$

which is exactly the solution for the AR coefficients. This result confirms that the AR memory module optimally balances the dual goals of preserving predictive information and minimizing redundancy, providing a principled foundation for its use in AR-KAN.

This adaptability endows AR-KAN with stronger generalization across diverse temporal patterns. The linear filters capture data-specific short-term dynamics, while the nonlinear KAN component models higher-order, nonlinear interactions. Together, they form a powerful hybrid that balances interpretability, efficiency, and expressiveness in time series forecasting.

IV. EXPERIMENTS

We conduct experiments in two parts to demonstrate both the effectiveness and generalizability of AR-KAN. First, we perform experiments on noisy almost-periodic functions to show that modern models fall short of traditional ARIMA models in terms of spectral analysis, while our AR-KAN achieves performance comparable to ARIMA. Then, we extend the evaluation to real-world datasets from Rdatasets[40], and observe that AR-KAN achieves the best performance on 72% of datasets. The few cases where it underperforms mostly involve weak or absent periodicity, which are inherently hard to predict without prior knowledge. For strongly periodic data, AR-KAN shows a clear and consistent advantage.

A. Noisy Almost Periodic Functions

We construct noisy almost-periodic functions by superimposing 2 trigonometric waves with incommensurate frequencies and adding Gaussian noise:

$$f_1(t) = \cos(2t) + \cos(2\pi t) + \text{noise}, \tag{18}$$

$$f_2(t) = \sin(3t) + \sin(2et) + \text{noise}, \tag{19}$$

TABLE II: Test loss (MSE) of various models on Rdatasets with periodicity strength

Datasets	Periodicity Strength	ARIMA	AR-KAN	AR-MLP	KAN	MLP	LSTM	FAN	FNO	LLMTime
airpass_ts	41.28%	0.3329	**0.0706**	0.0871	0.3046	0.3025	0.4249	0.5163	0.6982	0.1937
goog200_ts	34.24%	4.7135	**0.1228**	0.8096	3.6632	3.5888	3.2584	3.0580	7.9012	1.1351
euretail_ts	18.39%	0.4967	0.9964	1.3328	1.1984	0.4226	1.6740	1.1469	**0.1821**	1.5009
ausbeer_ts	14.63%	0.0418	**0.0357**	0.0741	0.1031	0.5102	0.0692	0.0802	0.1114	0.0436
h02_ts	13.31%	0.2726	**0.1263**	0.1782	1.3708	0.5258	0.2103	0.6003	0.8209	0.1371
BJsales_ts	10.08%	0.3241	**0.0032**	0.0261	0.0358	0.7849	0.0643	0.2393	1.0370	0.0131
a10_ts	6.36%	0.1441	**0.1353**	0.4775	2.5033	2.2638	0.8809	0.4913	0.3851	0.3457
hsales2_ts	4.20%	0.5781	**0.5232**	0.6301	2.1212	0.8286	1.7787	1.7065	0.8850	0.5667
co2_ts	3.69%	0.0218	**0.0014**	0.0064	0.3079	0.0460	0.1640	0.1584	0.1963	0.0109
hyndsight_ts	2.61%	0.8729	**0.2471**	0.3961	1.5734	0.4892	0.5929	0.6164	0.6793	0.4510
bricksq_ts	1.33%	0.2080	**0.0502**	0.0823	0.2542	0.2769	0.2961	0.9625	0.2607	0.2541
elecequip_ts	1.25%	0.3159	0.1528	0.2573	**0.1346**	0.5538	0.8984	0.7761	0.4870	1.4010
elecdaily_mts	1.16%	0.4331	**0.2123**	0.2573	0.4410	0.5366	0.6792	0.8981	0.5919	0.6127
gtemp_both_ts	0.50%	2.2374	**0.2936**	0.5328	3.2225	2.2946	1.6629	2.8678	1.6660	5.0938
discoveries_ts	0.22%	1.6030	2.1695	2.3091	1.7269	1.6264	1.7949	1.0153	**0.8469**	1.2922
elec_ts	0.16%	0.2731	0.0069	**0.0060**	0.0930	0.0436	0.1833	0.3258	0.0625	0.0727
economics_df_ts	0.00%	3.5659	**0.0845**	0.4398	2.3047	1.8717	2.2520	1.8607	7.7670	1.6490
auscafe_ts	0.00%	0.3301	0.3813	**0.1180**	2.6312	0.7564	0.3746	1.4820	3.4769	0.4463

Note: Bold numbers indicate the **minimum** value in each row. Rows are shaded in red when periodicity is present ($\geq 0.5\%$) and in blue when periodicity is weak ($< 0.5\%$).
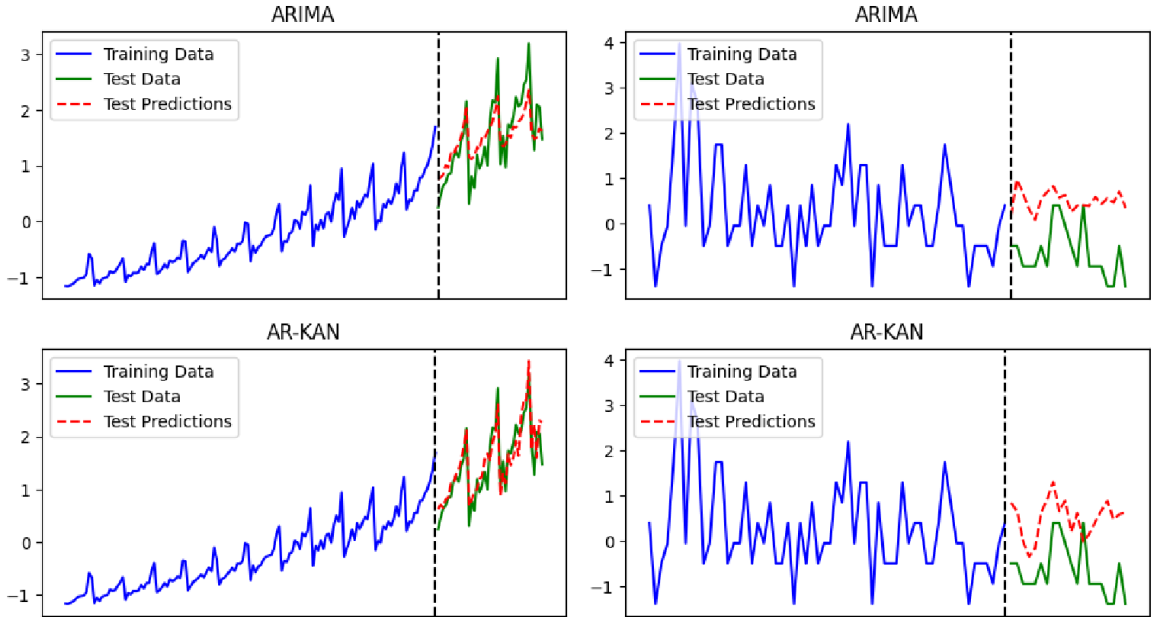

Fig. 4: Performance of ARIMA and AR-KAN on two different types of time series in Rdatasets. the left column shows results on a10_ts (a highly periodic series), and the right column shows results on discoveries_ts (a nearly non-periodic series).

where the noise is sampled from a zero-mean Gaussian distribution with variance σ^2. Almost-periodic functions like this are of particular significance in the development of harmonic analysis, and they form the basis of generalized harmonic analysis (GHA) as formulated by Wiener[2].

We vary the noise level σ from 0.1 to 0.4 and compare the performance of ARIMA and 9 neural models. The results are shown in TABLE I. Typically, the outcomes of certain experiments ($\sigma = 0.4$) produced by ARIMA, AR-KAN, and FAN are shown in Fig. 3.

Experimental results show that for almost-periodic functions, all 7 existing neural networks perform worse than ARIMA, including FNO and FAN, both of which are designed

specifically for spectral learning. As illustrated in Fig. 3, FAN is only able to capture the rough trend of the signal but fails to reconstruct fine-grained details. In contrast, the AR-KAN achieves excellent performance comparable to ARIMA. It inherits the strong spectral analysis capabilities of autoregressive models while also benefiting from the KAN's near absence of spectral bias, enabling it to handle the intricate details of the time series effectively.

This combination of strengths makes AR-KAN particularly suitable for data with complex frequency structures. The results highlight the effectiveness of our architecture in bridging the gap between traditional statistical methods and modern neural networks.

B. Rdatasets

We further evaluate AR-KAN on real-world series from Rdatasets[40]. For each dataset, we quantify its *Periodicity Strength* as the ratio of the energy of the seasonal component (obtained by STL decomposition[43]) to the total energy of the original series:

$$\text{Periodicity Strength} = \frac{\|x_{\text{seasonal}}\|_2^2}{\|x\|_2^2}.$$

The period used in STL decomposition is determined by the largest nonzero-lag peak in the series' autocorrelation function. Our results in TABLE II show that AR-KAN achieves the best performance on 72% of datasets. Moreover, its advantage grows with increasing Periodicity Strength, indicating that AR-KAN excels on series with clear or strong periodic components. In contrast, its few underperforming cases correspond to datasets with weak or nearly absent periodicity, which are inherently hard to forecast without additional prior knowledge and remain challenging for all competing methods. They are illustrated in Fig. 4. By the way, Fourier-based models fail to generalize despite their spectral priors, and other neural baselines show similar limitations.

LLM-based methods such as LLMTime[42] approach ARIMA[41] in performance but still fall short of AR-KAN, indicating that LLMs are not yet mature for time series forecasting. Both LLMs and neural networks struggle to capture frequency structure, whereas AR offers a statistical view for genuine spectral analysis. By combining this frequency-aware modeling with KAN's nonlinear expressivity, AR-KAN achieves robust, domain-general performance.

V. CONCLUSION

In this paper, we reveal that existing neural networks struggle with spectral analysis and often underperform ARIMA on almost-periodic functions. Guided by the Universal Myopic Mapping Theorem, we propose AR-KAN, which combines ARIMA's autoregressive memory with KAN's nonlinear expressivity. Experiments show that AR-KAN matches ARIMA on almost-periodic functions and outperforms baselines on 72% of real-world datasets, with its advantage growing on series with clear periodic patterns. These results highlight AR-KAN as a robust and unified framework for time series forecasting.

APPENDIX A
DATA SAMPLING AND EVALUATION PROTOCOL

In the *Noisy Almost Periodic Functions* experiment, the temporal variable t ranges from 0 to 8π, and a total of 500 samples are uniformly collected over this interval. The dataset is split into training and testing sets with an 80/20 ratio: the first 80% of the sequence is used for training, while the remaining 20% is reserved for testing.

For the *Rdatasets* experiment, all time series are standardized based on their mean and standard deviation. Then also apply the 80/20 split strategy: the training set consists of the first 80% of each sequence, and the testing set consists of the final 20%.

APPENDIX B
MODEL ARCHITECTURE AND CONFIGURATION

models	architecture and configuration
ARIMA	p = 20, d = 0 or 1, q = 1 or 2
KAN	width = [20,50,1], grid=3, k=3
MLP	width = [20, 128, 256, 128, 1]
Transformer	feature_dimension = 64, nhead=4, encoder_layers = 2, feedforward_dimension = 128
LSTM	input_size=1, hidden_size=64, num_layers=2, output_size=1
Mamba	input_dim=1, d_model=48, d_state=32, d_conv=20, n_layers=5
FAN	input_dim=20, output_dim=1, hidden_dim=2048, num_layers=5, p_ratio=0.25
FNO	input_dim=20, output_dim=1, modes=8, channels=32, fourier_layers = 2
LLMTime	DeepSeek-V3, experiment_times = 10

REFERENCES

[1] G. E. P. Box, G. M. Jenkins, G. C. Reinsel, and G. M. Ljung, *Time Series Analysis: Forecasting and Control*, 5th ed. Hoboken, New Jersey: John Wiley & Sons Inc., 2015.

[2] N. Wiener, *Extrapolation, interpolation, and smoothing of stationary time series: with engineering applications*. The MIT Press, 1949.

[3] C. Fernández-Pérez, J. Tejada, and M. Carrasco, "Multivariate time series analysis in nosocomial infection surveillance: a case study," *International Journal of Epidemiology*, vol. 27, no. 2, pp. 282–288, 4 1998. [Online]. Available: https://doi.org/10.1093/ije/27.2.282

[4] T. Wang, R. Beard, J. Hawkins, and R. Chandra, "Recursive deep learning framework for forecasting the decadal world economic outlook," *IEEE Access*, vol. 12, pp. 152 921–152 944, 1 2024. [Online]. Available: https://doi.org/10.1109/access.2024.3472859

[5] M. Singh, V. S. B, N. Acharya, A. Grover, S. A. Rao, B. Kumar, Z.-L. Yang, and D. Niyogi, "Short-range forecasts of global precipitation using deep learning-augmented numerical weather prediction," 6 2022. [Online]. Available: https://arxiv.org/abs/2206.11669

[6] Y. Deng, S. Liu, Z. Wang, Y. Wang, Y. Jiang, and B. Liu, "Explainable time-series deep learning models for the prediction of mortality, prolonged length of stay and 30-day readmission in intensive care patients," *Frontiers in Medicine*, vol. 9, 9 2022. [Online]. Available: https://doi.org/10.3389/fmed.2022.933037

[7] G. E. P. Box and G. M. Jenkins, "Some recent advances in forecasting and control," *Journal of the Royal Statistical Society. Series C (Applied Statistics)*, vol. 17, no. 2, pp. 91–109, 1968.

[8] B. Lim and S. Zohren, "Time-series forecasting with deep learning: a survey," *Philosophical Transactions of the Royal Society A Mathematical Physical and Engineering Sciences*, vol. 379, no. 2194, p. 20200209, 2 2021. [Online]. Available: https://doi.org/10.1098/rsta.2020.0209

[9] R. Csordás, C. Potts, C. D. Manning, and A. Geiger, "Recurrent Neural Networks Learn to Store and Generate Sequences using Non-Linear Representations," 8 2024. [Online]. Available: https://arxiv.org/abs/2408.10920

[10] I. A. Gheyas and L. S. Smith, "A neural network approach to time series forecasting," 2009. [Online]. Available: https://api.semanticscholar.org/CorpusID:2266156

[11] L. R. Medsker, L. Jain *et al.*, "Recurrent neural networks," *Design and applications*, vol. 5, no. 64-67, p. 2, 2001.

[12] S. Hochreiter and J. Schmidhuber, "Long Short-Term memory," *Neural Computation*, vol. 9, no. 8, pp. 1735–1780, 11 1997. [Online]. Available: https://doi.org/10.1162/neco.1997.9.8.1735

[13] A. Vaswani, N. Shazeer, N. Parmar, J. Uszkoreit, L. Jones, A. N. Gomez, L. Kaiser, and I. Polosukhin, "Attention is All you Need," *arXiv (Cornell University)*, vol. 30, pp. 5998–6008, 6 2017. [Online]. Available: https://arxiv.org/pdf/1706.03762v5

[14] Q. Wen, T. Zhou, C. Zhang, W. Chen, Z. Ma, J. Yan, and L. Sun, "Transformers in Time Series: A survey," 2 2022. [Online]. Available: https://arxiv.org/abs/2202.07125

[15] H. Zhou, S. Zhang, J. Peng, S. Zhang, J. Li, H. Xiong, and W. Zhang, "Informer: Beyond efficient transformer for long sequence Time-Series forecasting," *Proceedings of the AAAI Conference on Artificial Intelligence*, vol. 35, no. 12, pp. 11106–11115, 5 2021. [Online]. Available: https://doi.org/10.1609/aaai.v35i12.17325

[16] A. Gu and T. Dao, "Mamba: Linear-Time Sequence Modeling with Selective State Spaces," 12 2023. [Online]. Available: https://arxiv.org/abs/2312.00752

[17] Z. Liu, Y. Wang, S. Vaidya, F. Ruehle, J. Halverson, M. Soljačić, T. Y. Hou, and M. Tegmark, "Kan: Kolmogorov-arnold networks," 2024.

[18] Y. Lu and F. Zhan, "Kolmogorov Arnold Networks in Fraud Detection: Bridging the gap between theory and practice," 8 2024. [Online]. Available: https://arxiv.org/abs/2408.10263

[19] M. Jin, S. Wang, L. Ma, Z. Chu, J. Y. Zhang, X. Shi, P.-Y. Chen, Y. Liang, Y.-F. Li, S. Pan, and Q. Wen, "Time-LLM: Time series Forecasting by reprogramming large language models," 10 2023. [Online]. Available: https://arxiv.org/abs/2310.01728

[20] M. Tancik, P. P. Srinivasan, B. Mildenhall, S. Fridovich-Keil, N. Raghavan, U. Singhal, R. Ramamoorthi, J. T. Barron, and R. Ng, "Fourier features let networks learn high frequency functions in low dimensional domains," *Neural Information Processing Systems*, vol. 33, pp. 7537–7547, 6 2020. [Online]. Available: https://proceedings.neurips.cc/paper/2020/file/55053683268957697aa39fba6f231c68-Paper.pdf

[21] M. Kim, Y. Hioka, and M. Witbrock, "Neural fourier modelling: a highly compact approach to Time-Series analysis," 10 2024. [Online]. Available: https://arxiv.org/abs/2410.04703

[22] Y. Dong, G. Li, Y. Tao, X. Jiang, K. Zhang, J. Li, J. Deng, J. Su, J. Zhang, and J. Xu, "FAN: Fourier Analysis Networks," 10 2024. [Online]. Available: https://arxiv.org/abs/2410.02675

[23] S. Guan, K.-T. Hsu, and P. V. Chitnis, "Fourier Neural Operator network for fast photoacoustic wave simulations," *Algorithms*, vol. 16, no. 2, p. 124, 2 2023. [Online]. Available: https://arxiv.org/abs/2108.09374

[24] A. S. Besicovitch, "Almost periodic functions," *Nature*, vol. 131, no. 3307, p. 384, 3 1933. [Online]. Available: https://doi.org/10.1038/131384b0

[25] G. B. Folland, "Fourier analysis and its applications," *Choice Reviews Online*, vol. 30, no. 03, pp. 30–1562, 11 1992. [Online]. Available: https://doi.org/10.5860/choice.30-1562

[26] L. Amerio and G. Prouse, *Almost-Periodic functions and functional equations*, 1 1971. [Online]. Available: https://doi.org/10.1007/978-1-4757-1254-4

[27] R. H. Shumway and D. S. Stoffer, *Time Series Analysis and its applications*, 11 2010. [Online]. Available: https://doi.org/10.1007/978-1-4419-7865-3

[28] J. F. Torres, D. Hadjout, A. Sebaa, F. Martínez-Álvarez, and A. Troncoso, "Deep learning for Time Series Forecasting: A survey," *Big Data*, vol. 9, no. 1, pp. 3–21, 12 2020. [Online]. Available: https://doi.org/10.1089/big.2020.0159

[29] I. Sandberg and L. Xu, "Uniform approximation of multidimensional myopic maps," *IEEE Transactions on Circuits and Systems I Fundamental Theory and Applications*, vol. 44, no. 6, pp. 477–500, 6 1997. [Online]. Available: https://doi.org/10.1109/81.585959

[30] I. W. Sandberg and L. Xu, "Uniform Approximation of Discrete-Space Multidimensional Myopic Maps," *Circuits Systems and Signal Processing*, vol. 16, no. 3, pp. 387–403, 5 1997. [Online]. Available: https://doi.org/10.1007/bf01246720

[31] Q. Hong, J. W. Siegel, Q. Tan, and J. Xu, "On the Activation Function Dependence of the Spectral Bias of Neural Networks," 8 2022. [Online]. Available: https://arxiv.org/abs/2208.04924

[32] A. B. Givental, B. A. Khesin, J. E. Marsden, A. N. Varchenko, O. Y. Viro, and V. M. Zakalyukin, *On the representation of functions of several variables as a superposition of functions of a smaller number of variables*, 1 2009. [Online]. Available: https://doi.org/10.1007/978-3-642-01742-1_5

[33] Y. Wang, J. W. Siegel, Z. Liu, and T. Y. Hou, "On the expressiveness and spectral bias of KANs," 10 2024. [Online]. Available: https://arxiv.org/abs/2410.01803

[34] H. Shen, C. Zeng, J. Wang, and Q. Wang, "Reduced effectiveness of kolmogorov-arnold networks on functions with noise," in *ICASSP 2025 - 2025 IEEE International Conference on Acoustics, Speech and Signal Processing (ICASSP)*, 2025, pp. 1–5.

[35] C. Zeng, J. Wang, H. Shen, and Q. Wang, "KAN versus MLP on Irregular or Noisy Functions," 8 2024. [Online]. Available: https://arxiv.org/abs/2408.07906

[36] G. U. Yule, "VII. On a method of investigating periodicities disturbed series, with special reference to Wolfer's sunspot numbers," *Philosophical Transactions of the Royal Society of London Series A Containing Papers of a Mathematical or Physical Character*, vol. 226, no. 636-646, pp. 267–298, 1 1927. [Online]. Available: https://doi.org/10.1098/rsta.1927.0007

[37] G. T. Walker, "On periodicity in series of related terms," *Proceedings of the Royal Society of London Series A Containing Papers of a Mathematical and Physical Character*, vol. 131, no. 818, pp. 518–532, 6 1931. [Online]. Available: https://doi.org/10.1098/rspa.1931.0069

[38] J. A. Moorer, "About this reverberation business," *Computer Music Journal*, vol. 3, no. 2, p. 13, 6 1979. [Online]. Available: https://doi.org/10.2307/3680280

[39] B. De Vries and J. C. Principe, "The gamma model—A new neural model for temporal processing," *Neural Networks*, vol. 5, no. 4, pp. 565–576, 7 1992. [Online]. Available: https://doi.org/10.1016/s0893-6080(05)80035-8

[40] V. Arel-Bundock, "Rdatasets: A collection of datasets originally distributed in r packages," GitHub. [Online]. Available: https://github.com/vincentarelbundock/Rdatasets

[41] R. Cao and Q. Wang, "An evaluation of standard statistical models and llms on time series forecasting," in *2024 IEEE International Conference on Future Machine Learning and Data Science (FMLDS)*, 2024, pp. 533–538.

[42] N. Gruver, M. Finzi, S. Qiu, and A. G. Wilson, "Large language models are Zero-Shot time series forecasters," 10 2023. [Online]. Available: https://arxiv.org/abs/2310.07820

[43] R. B. Cleveland, W. S. Cleveland, J. E. McRae, I. Terpenning *et al.*, "Stl: A seasonal-trend decomposition," *J. off. Stat*, vol. 6, no. 1, pp. 3–73, 1990.